Efficient and Reusable Activated Carbon from *Aframomum angustifolium* Fruits' Shells for Removal of Ceftriaxone from Aqueous Solution: Adsorption Isotherms, Kinetics, and Thermodynamics Studies

Baraka Alfaksad Kasazi, Alinanuswe Joel Mwakalesi*, and Emmy Solomon Lema

Department of Chemistry and Physics, College of Natural and Applied Sciences, Sokoine University of Agriculture, P.O. Box 3038, Mazimbu-Morogoro, Tanzania

* ***Corresponding author:***

tel: +255-718057968
email: mwakalesi@sua.ac.tz

Received: June 17, 2025
Accepted: November 26, 2025

DOI: 10.22146/ijc.108042

Abstract: *The accumulation of ceftriaxone antibiotics in aquatic systems is a growing global concern due to their potential risks to human and ecological health. The current study investigates the synthesis, characterization, and application of activated carbon (AC-FPAA-H_3PO_4) made from the shells of* Aframomum angustifolium *fruits. AC-FPAA-H_3PO_4 was synthesized using chemical activation (H_3PO_4, 4 M) followed by pyrolysis at 600 °C for 1 h and characterized using BET, FTIR, and SEM-EDX. AC-FPAA-H_3PO_4 exhibited a surface area of 1895.6 m^2/g, which allowed for its reuse in 5 consecutive cycles without requiring active site regeneration. The optimal removal efficiency (97.8%) was achieved at pH 2, 298.15 K, 100 rpm, 20 g/L adsorbent dosage, and 200 mg/L ceftriaxone concentration. The adsorption process was described by Langmuir (R^2 = 0.9862) and Freundlich (R^2 = 0.9833) isotherms, and the kinetics were fitted to the pseudo-second-order model. The adsorption was spontaneous (ΔG = −6.80 kJ/mol) and exothermic (ΔH = −4.43 kJ/mol), with increased randomness at the solid-solution interface (ΔS = 7.69 J/mol K). The adsorbent demonstrated high efficiency in removing ceftriaxone from real water samples, including river water (99.36%) and well water (96.92%). The findings suggest AC-FPAA-H_3PO_4 is a promising adsorbent for removing ceftriaxone from an aqueous environment.*

Keywords: Aframomum angustifolium*; biowaste; activated carbon; ceftriaxone; antibiotic*

■ INTRODUCTION

Pharmaceutical compounds are regarded as emerging environmental pollutants due to their high availability and widespread use [1]. Antibiotics are estimated to account for 16.3% of the total medicine consumption [2]. Many of these are environmentally persistent and can accumulate in soil, water, and even food crops [3-4]. Some antibiotics are indeed degraded in the body, while others are excreted unchanged [5]. Antibiotics enter the aquatic environment through various routes, including human excretion in hospitals and households, hospital effluents, and pharmaceutical industrial effluents that are discharged into wastewater. Additionally, animal husbandry activities and improper disposal of antibiotic drugs can lead to their accumulation in the aquatic environment through runoff water [6]. Furthermore, leaching into surface or groundwater from solid waste containing expired drugs, such as landfill leachate, contributes to the possible route of antibiotic contaminants in the aquatic environment [7]. The presence of antibiotics in the aquatic environment poses a risk to the ecosystems and human health [8]. Health problems associated with the accumulation of antibiotics in the environment include cancer, neurotoxicity, mental disorders, and impaired immune function [9]. The development of antibiotic resistance genes is also an emerging challenge linked to the accumulation of antibiotic residues in aquatic environments [10].

Cephalosporin is a class of widely used antibiotics due to their strong bactericidal action and broad

antibacterial spectrum. Consequently, it is employed to treat various bacterial infections, including acute pneumonia, bone and joint infections, respiratory infections, urinary tract infections, soft tissue infections, skin infections, and bloodstream infections. However, the accumulation of cephalosporin in the environment is a growing concern due to their toxic effects on ecosystems, even at low doses [11]. Ceftriaxone is a third-generation cephalosporin antibiotic widely used to treat a broad range of bacterial infections, including respiratory tract infections, skin infections, urinary tract infections, gonorrhea, and meningitis [12]. It is administered intravenously or intramuscularly in clinical settings and excreted in unchanged form [13]. Ceftriaxone is relatively stable in an aquatic environment and does not degrade easily. Thus, improper disposal of antibiotics and leaching from landfill leachate may contribute to their viability in the aqueous environment. The highest ceftriaxone concentration of 8.5×10^{-5} ppm was reported in the Tigris River in Iraq [14]. The complete removal of ceftriaxone from wastewater is difficult due to its complex molecular structure [15]. As a consequence, ceftriaxone resistance to bacteria as serious issues on human health globally has been reported [16].

Different water treatment methods, including adsorption, chemical oxidation, photochemical degradation, ozonation, ion exchange, photocatalysis, and biological processes, have been developed to remove ceftriaxone from aqueous solutions. However, most of these methods face challenges such as continuous chemical consumption, sludge generation, and high maintenance costs, while biological methods suffer from poor biodegradation efficiency [15]. The adsorption method is the most preferred technique for removing organic contaminants, such as ceftriaxone, due to its effectiveness, affordability, versatility, and ability to be regenerated [17].

Activated carbon (AC) is a highly effective adsorbent for removing different contaminants due to its high surface area, porous structure, and versatile surface chemistry [18]. Traditionally, AC is produced from non-renewable sources, such as coal, which involves significant energy consumption, high costs, resource depletion, health and safety concerns, and environmental impacts, including land degradation and greenhouse gas emissions from mining and processing [19]. Therefore, the current interest is growing in developing AC from renewable and sustainable materials, particularly agricultural and forestry biowastes. These offer potentially more sustainable, environmentally friendly, and cost-effective solutions [20]. Utilizing biowastes also reduces greenhouse gas emissions associated with their decomposition upon disposal in landfills [21]. Most agricultural products are rich in cellulose, hemicellulose, and lignin, making them suitable AC precursors due to their abundance of functional groups, such as hydroxyl, carboxylic, and phenolic [22]. These groups enhance AC's selectivity for various chemical contaminants through interactions [23].

A. angustifolium is a tropical plant in Africa bearing edible fruits consumed in countries like Tanzania, Uganda, and the Democratic Republic of Congo [24]. The fruits' shells of *A. angustifolium* (FPAA) are discarded as bio-waste. The shells, like other biomass, are rich in cellulose, hemicellulose, and lignin, making them suitable for AC production [25]. However, there is limited information on utilizing the waste for AC synthesis. Thus, this study reports on the synthesis and application of AC derived from FPAA for removing cephalosporins from aqueous environments, using ceftriaxone as a model compound. The use of a novel and sustainable method for removing this persistent antibiotic using AC derived from this bio-waste is presented in the current study. The transformation of abundant agricultural waste into high-surface-area carbon valorizes a low-value byproduct, aligning with green chemistry and circular economy principles, reduces waste generation, and contributes to the development of affordable, effective adsorbents for water purification.

■ EXPERIMENTAL SECTION

Materials

FPAA, $NaH_2PO_4{\cdot}2H_2O$ (98%, Fisher Scientific International), $Na_2HPO_4{\cdot}2H_2O$ (99.5%, Riedel-deHaën), H_3PO_4 (85%, Loba Chemie, Mumbai, India), CH_3CH_2OH (Scharlau, Spain), $NaHCO_3$ (99.7%, Loba Chemie, Mumbai, India), NaOH (97%, Loba Chemie, Mumbai,

India), NaCl (99.5%, Loba Chemie, Mumbai, India), HCl (37%, Loba Chemie, Mumbai, India), I_2 (99.5%, Lab-Tech Chemicals, India), soluble starch (Lab-Tech Chemicals, India), $Na_2S_2O_3{\cdot}5H_2O$ (99%, Lab-Tech Chemicals, India), KI (99%, Molaton Scientific, India), and ceftriaxone (Theon pharmaceuticals ltd, Villi Saini Majra, Tehsil Nalagarh, Distt. Solan (HP), 174, 101, India) were used in this work.

Instrumentation

Several instruments were used in this study, including a 6715 UV-vis spectrophotometer (JENWAY), a Muffle furnace, a shaker from Sheldon Manufacturing, Inc., 300 N 26th Cornelius, OR97113, a blender, a pH meter, Quantachrome NovaWin©1994-2013, a scanning electron microscope (SEM, JOEL, JSM-6610LV), and an IRAffinity-1S Fourier transform infrared spectrophotometer (FTIR, Shimadzu).

Procedure

Sample collection and preparation

A. angustifolium fruits, collected from Kasulu district, were washed, peeled, and sun-dried for 7 days. The dried samples were then transported to the Sokoine University of Agriculture laboratory in Morogoro, Tanzania. They were washed with distilled water, dried, and ground into a fine powder using a blender. The resultant powder was then sieved through a 125 μm mesh and stored in polyethylene bags.

Preparation of AC

The AC was prepared using previously reported procedures with minor modifications [26]. Briefly, AC was prepared by soaking 30 g of powdered shells (FPAA) in 500 mL of 4 M H_3PO_4 for 24 h. The mixture was filtered through a 0.7 μm Whatman filter paper, placed in a crucible, and dried in an oven at 110 °C for 36 h. The dried material was carbonized at 600 °C for 1 h to obtain AC, then cooled for an additional 1 h. The resulting AC was ground with a mortar and pestle, soaked in a 20% ethanol-water solution for 5 h with stirring (100 rpm, room temperature), and then filtered. To neutralize the residual acid from phosphoric acid activation (AC-FPAA-H_3PO_4), the carbon was soaked in 500 mL of a 1% $NaHCO_3$ solution for 1 h. The AC-FPAA-H_3PO_4 was then washed with distilled water until the pH was constant at 7. After oven-drying at 105 °C for 12 h and cooling, the AC-FPAA-H_3PO_4 was reground using a mortar and pestle, and stored in a centrifuge bottle inside a polyethylene bag for characterization and adsorption experiments.

Adsorbent characterization

Percentage yield. The percentage yield of AC-FPAA-H_3PO_4 was calculated using Eq. (1), where the mass ratio of the produced AC to the washed, dried, and ground FPAA precursor material was multiplied by 100;

$$\text{Percentage yield } (\%) = \frac{w_1}{w_0} \times 100\% \quad (1)$$

where w_0 is the mass of the washed, dried, and ground sample of FPAA, and w_1 is the mass of AC produced.

Bulk density. The bulk density of AC-FPAA-H_3PO_4 was determined by weighing an empty 10 mL measuring cylinder, filling it to the mark with AC, and reweighing. The bulk density was calculated using Eq. (2);

$$\text{Bulky density} = \frac{W_{AC}}{V_{AC}} \quad (2)$$

where W_{AC} is the mass of the AC, and V_{AC} is the cylinder volume packed with AC.

Moisture content. Moisture content (hygroscopic property) was determined by weighing 1 g of AC-FPAA-H_3PO_4 (w_2) in a crucible (w_0) using a digital balance, drying at 105 °C for 1 h, and reweighing the crucible with the sample (w_1). Moisture content was calculated using Eq. (3).

$$\text{Moisture content } (\%) = \frac{w_0 - w_1}{w_2} \times 100\% \quad (3)$$

Ash content. Ash content was determined by weighing 1 g of AC-FPAA-H_3PO_4 (w_3) in a crucible (w_1), heating in a furnace at 600 °C for 2 h, and reweighing the crucible with residue (w_2). Ash content was calculated using Eq. (4).

$$\text{Ash content } (\%) = \left(\frac{w_1 - w_2}{w_3} \right) \times 100\% \quad (4)$$

Iodine number. Iodine number was determined by titration, where 0.1 g of AC-FPAA-H_3PO_4 was added to 100 mL of 0.05 M I_2 solution, shaken at 150 rpm (25 °C, 30 min), and filtered. For the sample titration, 10.0 mL of the filtrate was mixed with 5.0 mL of KI and 1.0 mL of

HCl, and then titrated with a standardized 0.1 M $Na_2S_2O_3$ solution until a pale-yellow color was observed. After adding 2.0 mL of starch indicator, the titration continued until the solution was colorless. A blank titration was performed using 10.0 mL of the original iodine solution. The iodine number was calculated using Eq. (5);

$$\text{Iodine number} = \frac{(B-S)\times M\times 10000}{W} \quad (5)$$

where B is the volume of sodium thiosulphate used in the absence of AC (mL), *S* is the volume of thiosulphate used in titration in the presence of AC (mL), M is the normality of sodium thiosulphate solution, and W is the mass of AC used (g).

Determination of the point of zero charge (pH_{pzc}) of AC-FPAA-H_3PO_4. The point of zero charge was determined using the batch equilibrium method (pH drift method). Solutions ranging from pH 2 to pH 12 were prepared using 0.1 M NaCl as the background electrolyte, with pH adjustment using 0.1 M HCl and 0.1 M NaOH. Then, 30 mg of FPAA-AC was added to 40 mL aliquots of each pH solution. The mixtures were shaken for 24 h at 100 rpm and 25 °C.

BET surface area. The BET surface analysis was conducted using Quantachrome NovaWin©1994-2013, Quantachrome Instrument v11.03 to determine the specific surface area of the adsorbent. The AC and its raw materials, each at 0.0749 g, were used for the analysis.

SEM and energy-dispersive X-ray (EDX) spectroscopy analysis. The surface morphology and elemental composition of the precursor materials (FPAA) and AC-FPAA-H_3PO_4 were analyzed using SEM before and after adsorption. A small amount of sample was sprinkled on a clean aluminum stub with carbon tape using a clean spatula. The stub was then placed in a sputter coater with a Pd/Au target. The stub was further placed on the SEM/EDS stage, secured, and pumped down to the vacuum.

FTIR analysis. The functional groups of the precursor materials (FPAA) and the adsorbent (AC-FPAA-H_3PO_4) were analyzed using a FTIR. A small amount of AC was mixed with 100 mg of potassium bromide (KBr) in a mortar and pestle. The mixture was compressed in the machine to obtain a pellet sample, which was then placed in a cell for analysis.

Adsorption experiments

Ceftriaxone solution (1,000 mg/L) was prepared using phosphate buffer solution, and then a serial dilution was made to obtain the required concentration**.** The known mass of AC-FPAA-H_3PO_4 was added to 5 mL of a known concentration of ceftriaxone solution, and the mixture was shaken at 100 rpm for 1 h. Thereafter, the mixture of AC and ceftriaxone solution was filtered using 0.7 μm Whatman filter paper to obtain a clear solution, which was then used for measuring the ceftriaxone concentration. The concentration of ceftriaxone before and after adsorption was determined by scanning the solution using UV-vis spectrometer. The optimization of parameters, including pH, temperature, ceftriaxone concentration, and dosage of AC-FPAA-H_3PO_4, was studied at an agitation speed of 100 rpm and a contact time of 1 h. The removal efficiency and adsorption capacity at equilibrium were calculated using Eq. (6) and (7), respectively;

$$RE\% = \frac{C_0 - C_e}{C_0}\times 100\% \quad (6)$$

$$q_e = (C_0 - C_e)\times\frac{v}{m} \quad (7)$$

where q_e is the adsorption capacity, RE% is the removal efficiency, C_0 is the initial concentration, C_e is the concentration of ceftriaxone at equilibrium, v is the volume of adsorbate solution, and m is the mass of adsorbent.

Adsorption isotherms

The Langmuir and Freundlich isotherm models were evaluated using adsorption data at ceftriaxone concentrations ranging from 20 to 1,000 mg/L, an adsorbent dose of 0.1 g/5 mL, a solution pH of 2, and a contact period of 1 h, which were determined to be optimal experimental conditions. Eq. (8) and (9) were applicable for the Langmuir equation, while Eq. (10) was applicable for the Freundlich model;

$$\frac{1}{q_e} = \frac{1}{q_{max}} + \frac{1}{K_L q_{max}}\times\frac{1}{C_e} \quad (8)$$

$$R_L = \frac{1}{1 + K_L q_{max}\times C_0} \quad (9)$$

$$\log q_e = \log K_F + \frac{1}{n}\times\log C_e \quad (10)$$

where C_0 is the initial concentration of ceftriaxone, q_e is the ceftriaxone concentration at equilibrium, C_e is the concentration of ceftriaxone at equilibrium, q_{max} is the ceftriaxone monolayer's maximum adsorption, K_L is the Langmuir constant which is related to energy of adsorption, R_L is the ceftriaxone and AC-FPAA-H_3PO_4 affinity, and K_F is the Freundlich constant, n is the Freundlich index which shows the degree of adsorption and surface heterogeneity.

Kinetics studies

A kinetics study was evaluated using adsorption at different times (from 0 to 480 s) at a 500 mg/L ceftriaxone concentration, 0.1 g/100 mL of adsorbent, 100 rpm, and 298.15 K. The four kinetic models (pseudo-first order, pseudo-second order, Elovich, and Weber's intraparticle diffusion) were evaluated using Eq. (11–14), respectively;

$$\log(q_e - q_t) = \log q_e - \frac{k_1 t}{2.303} \quad (11)$$

$$\frac{t}{q_t} = \frac{1}{k_2 q_e^2} + \frac{t}{q_e} \quad (12)$$

$$q_t = \frac{1}{\beta}\ln(\alpha\beta) + \frac{1}{\beta}\ln(t) \quad (13)$$

$$q_t = k_i t^{0.5} + C_i \quad (14)$$

where q_e is the amount adsorbate adsorbed at equilibrium (mg/g), q_t is the amount of adsorbate adsorbed at any time (mg/g), t is the adsorption time (s), k_1 is the first rate constant, k_2 is the second rate constant, α is the initial adsorption rate (mg/g min), β is desorption constant, which is related to the surface coverage and activation energy of chemisorption (mg/g), k_i is the intraparticle diffusion rate constant, and C_i is the thickness of boundary layer.

Thermodynamic study

Thermodynamic parameters were evaluated by conducting an adsorption experiment using a 20 mg/L ceftriaxone solution, a 20 g/L adsorbent dosage, 100 rpm, pH 2, and for 1 h at different temperatures (298.15, 308.15, 318.15, 328.15, and 338.15 K). The determination of enthalpy, Gibbs free energy, and entropy changes involved Eq. (15–17);

$$K = \frac{C_a}{C_e} \quad (15)$$

$$\Delta G = -RT\ln K \quad (16)$$

$$\ln K = \frac{\Delta S}{R} - \frac{\Delta H}{RT} \quad (17)$$

where K is the equilibrium constant, C_e is the adsorbate concentration remaining in the solution (mg/L), C_a is the adsorbate concentration adsorbed at equilibrium (mg/L), R is the universal gas constant, T is the temperature (K), ΔG is the change in Gibbs free energy, and ΔH is the enthalpy change, and ΔS is the entropy change.

■ RESULTS AND DISCUSSION

Adsorbent Characterization

Percentage yield, bulk density, moisture content, ash content, and iodine number of AC

The characterization results of the AC-FPAA-H_3PO_4 are presented in Table 1. The results revealed a carbon yield of 25.97%, a bulk density of 0.186 g/mL, a moisture content of 15%, an ash content of 2.88%, and an iodine number of 700 mg/g. The relatively low values of bulk density, ash content, and moisture content suggest that the material possesses desirable characteristics for broad adsorption applications. AC with ash content ranging from 1 to 20% is suitable for adsorbing various contaminants [27]. Therefore, the ash content of 2.88% confirms that the synthesized AC meets the quality standards for effective adsorption, including that of antibiotics. Moreover, the iodine number of 700 mg/g falls within the accepted range for high-quality AC (500–1200 mg/g), as reported by Ceyhan et al. [28]. This further indicates a favorable microporous structure, supporting its effectiveness in adsorbing small molecules such as ceftriaxone. These preliminary findings confirm that the AC-FPAA-H_3PO_4

Table 1. Yield, bulk density, moisture content, ash content, and iodine number of AC-FPAA-H_3PO_4

Parameter	Value	Standards	Reference
Carbon yield (%)	25.97	min 30%	[29]
Bulk density (g/mL)	0.186	0.30–0.35	[29]
Moisture content (%)	15	max 15	[30]
Ash content (%)	2.88	max 10	[30]
Iodine number (mg/g)	700	500–1200	[28]

prepared was suited for adsorption applications, and thus, it was used for subsequent experiments.

pH_{pzc} of AC-FPAA-H_3PO_4

The surface charge of an adsorbent plays a significant role in determining the nature of its interaction with a target analyte. The pH_{pzc} corresponds to the pH at which the number of positive and negative charges on the adsorbent surface is equal [31]. Thus, the pH_{pzc} of the synthesized AC-FPAA-H_3PO_4 was determined, and the results (Fig. 1) revealed a pH_{pzc} value of 4.5. This indicates that the surface of AC-FPAA-H_3PO_4 is electrically neutral at pH 4.5. At pH values below 4.5, the surface carries a net positive charge, while at pH values above 4.5, the surface becomes negatively charged. This behavior influences the electrostatic interactions between the adsorbent and charged species in solution. Similar pH_{pzc} values have been reported in previous studies for AC derived from mango peels (pH_{pzc} = 4.6) [32]. This comparison supports the characterization of AC-FPAA-H_3PO_4 as a viable adsorbent with predictable charge behavior across different pH levels.

BET analysis

The Brunauer-Emmett-Teller (BET) surface area provides a quantitative measure of the total surface area available for adsorption on a material. As shown in Table 2, the BET analysis revealed that the prepared AC-FPAA-H_3PO_4 exhibited a significantly higher surface area of 1895.646 m^2/g compared to its precursor material, FPAA, which had a surface area of 335.809 m^2/g. This considerable increase suggests that AC-FPAA-H_3PO_4 possesses a greater number of adsorption sites, thereby enhancing its adsorption potential for pollutant molecules [33]. AC with a surface area greater than 1,000 m^2/g has been reported to be efficient for removing various organic pollutants from aqueous solutions [34]. Additionally, the findings in the current study showed that the activation process resulted in an increase in total pore volume, average pore size, pore volume, pore diameter, and pore surface area (Table 2). The average pore radius increased from 0.522 nm in FPAA to 0.657 nm in AC-FPAA-H_3PO_4, indicating that the AC provides sufficient spatial accommodation for adsorbate molecules. Moreover, the pore volume nearly doubled, increasing from 1.186 to 2.292 cm^3/g, which further supports the enhanced adsorption capacity. The pore volume increased from 0.292 cm^3/g of the precursor materials (FPAA) to 1.653 cm^3/g of the adsorbent. As well, pore surface area increased from 185.874 cm^3/g of precursor material (FPAA) to 741.849 cm^3/g for the AC-FPAA-H_3PO_4. Therefore, the increased pore volume and surface area indicate that the adsorbent contains sites with a remarkable ability to capture and retain adsorbate molecules. The presence of a larger pore network facilitates faster diffusion of organic molecules into the adsorbent, improving the overall efficiency of the adsorption process. The nature of the adsorption isotherm shape suggests that the AC-FPAA-H_3PO_4 involves a type IV isotherm, as shown in Fig. S1. The reported type IV adsorption isotherms were previously

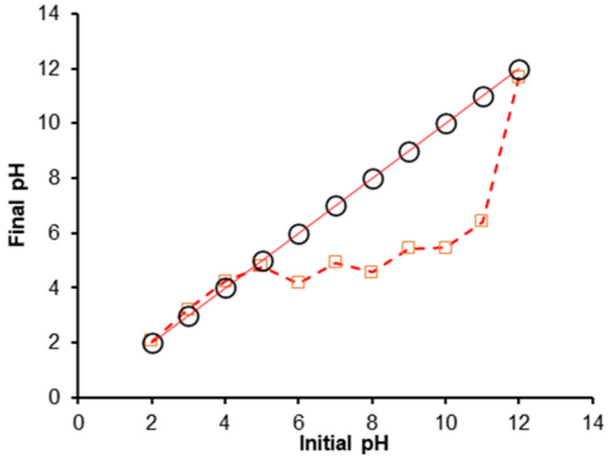

Fig 1. The pH_{pzc} plot of AC-FPAA-H_3PO_4

Table 2. BET surface area, average pore size, and total pore volume

Material	Surface area (m^2/g)	Average pore size (nm)	Total pore volume (cm^3/g)	Pore volume (cm^3/g)	Pore diameter (nm)	Pore surface area (m^2/g)
FPAA	335.809	0.522	1.186	0.292	1.6954	185.874
AC-FPAA-H_3PO_4	1895.646	0.657	2.292	1.653	1.7030	741.849

reported by others [35-36]. The observation indicates that the surface of the AC is characterized by the presence of mesopores. The presence of a large number of mesopores supports the large surface area presented earlier in this section. The pore size distribution (Fig. S2) revealed that the majority of pores were within the 2–50 nm size range, indicating the presence of mesopores.

SEM-EDX analysis

As shown in Fig. 2(a), FPAA exhibited irregular, large blocks and aggregations with smooth surfaces. However, the AC (Fig. 2(b)) transformed into rough aggregates with pores of varying diameters. This was probably developed due to the chemical activation and physical activation of the FPAA as a precursor material [37]. The destructed and clogged pore surfaces of the adsorbent were observed after adsorption (Fig. 2(c)). This was a possible indicator that ceftriaxone molecules were adsorbed into the pores of the adsorbent [17]. The findings also indicate that the pores were not completely filled with the adsorbed molecules. This is a possible indicator of the reusability of the fabricated AC without the need for regenerating the active sites.

Elemental compositions of the precursor material (FPAA), the adsorbent before adsorption (AC-FPAA-H_3PO_4), and the adsorbent after adsorption are shown in Fig. S3 and Table 3. The findings showed that FPAA precursor composition composed of C (49.96%), N (2.07%), O (46.72%), Mg (0.49%), P (0.18%), K (0.4%), Mn (0.06%), and Fe (0.05%) while the AC-FPAA-H_3PO_4 adsorbent composed of C (79.40%), N (11.12%), O (6.66%), P (2.43%), K (0.19%), Mn (0.09%), and Fe (0.09%). The increase in carbon content for the AC (49.96 to 79.40%) demonstrates that chemical activation with H_3PO_4 and physical activation at 600°C enhanced carbon formation [38]. The decrease in O (46.72 to 6.66%) further indicates the effective removal of volatile compounds during activation, producing a porous surface. The increase in N (2.07 to 11.12%) and P (0.18 to 2.43%) was also observed for the post-adsorption AC. After adsorption, the adsorbent also exhibited the presence of new elements, including S (0.20%) and Na (0.32%). The increase in N (11.12 to 11.80%) and O (6.66 to 9.39%) was possibly attributed to the adsorption of ceftriaxone.

FTIR analysis

The FTIR analysis was employed to investigate the surface chemistry of the precursor materials and AC. The results (Fig. 3 and Table S1) showed a broad peak at 3344 cm^{-1}, associated with O−H stretching vibrations in alcohols or phenols, and a sharp peak at 3660 cm^{-1},

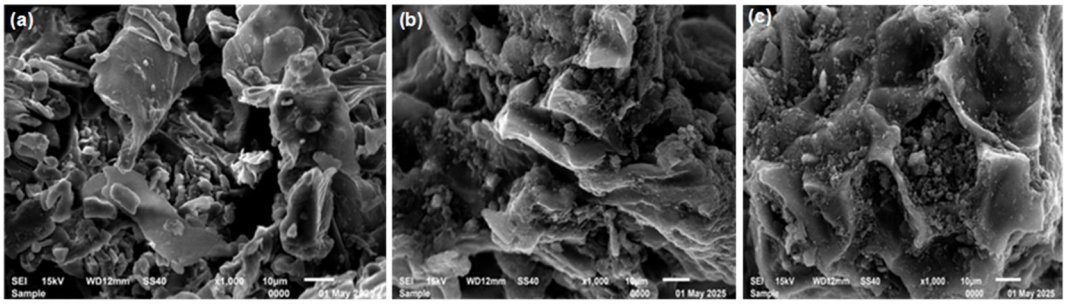

Fig 2. SEM images of (a) FPAA, (b) AC-FPAA-H_3PO_4 pre-adsorption, and (c) AC-FPAA-H_3PO_4 post-adsorption

Table 3. Elemental composition of precursor and AC before and after adsorption

Element	FPAA	Pre-adsorption AC-FPAA-H_3PO_4	Post-adsorption AC-FPAA-H_3PO_4
C	49.96	79.40	75.54
N	2.07	11.12	11.80
O	46.72	6.66	9.39
S	-	-	0.20
Cl	-	-	0.10

*elemental compositions are in weight percentage (wt.%)

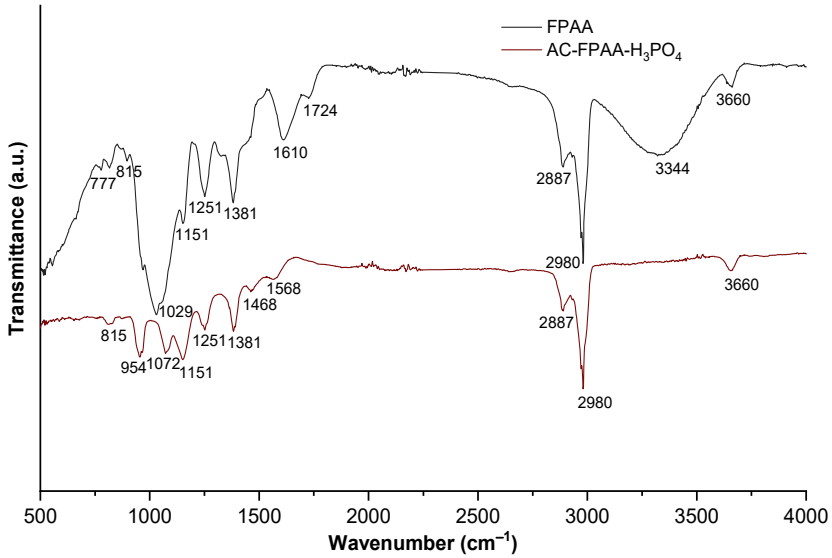

Fig 3. FTIR spectra of FPAA and AC-FPAA-H_3PO_4

attributed to free O–H groups. Peak observed at 1029 cm^{-1} was associated with C–O stretching vibration of anhydride, while the peak at 1251 cm^{-1} likely indicates C–O stretch of carboxylic acids. Additionally, peaks at 1381, 1610, and 1724 cm^{-1} correspond to bending vibrations of methyl (CH_3) or nitro (N=O) compounds, C=C groups, and C=O groups, respectively. Similar findings were previously reported by other researchers [38]. Conversely, the broad O–H peak (3344 cm^{-1}) was absent in the AC-FPAA-H_3PO_4 (Fig. 3), indicating functional group modification during the activation process. The adsorbent material also exhibited a peak at 954 cm^{-1}, which was related to the P–H bond [39]. It was not prominent in the precursor material (FPAA), further demonstrating functional group modification. Peaks at 1462 and 1568 cm^{-1} in AC-FPAA-H_3PO_4 were associated with the C=C bonds of aromatic rings. The similar findings were previously reported [40]. Peak at 1072 cm^{-1} for the AC-FPAA-H_3PO_4 is related to the phosphate oxide bond (P=O). The peak on AC-FPAA-H_3PO_4 at 954 cm^{-1} can also be associated with the phosphine bond (P–H bond). However, similar peaks in raw materials, and AC-FPAA-H_3PO_4 at 1151 cm^{-1} (stretch C–N), 1381 cm^{-1} (CH_3 or N=O bonds), 2980 cm^{-1} (C–H), and 3660 cm^{-1} (free O–H) were observed, highlighting the presence of functional groups in AC for supporting electrostatic interactions and hydrogen bonding with adsorbates. The distinct peaks at 1462 and 1568 cm^{-1} in AC-FPAA-H_3PO_4 likely indicate the presence of hydrocarbons associated with the C=C bonds of aromatic rings [39]. The presence of a weak peak at 500–850 cm^{-1} in the FTIR spectra of both raw material and AC-FPAA-H_3PO_4 also signifies =C–H bonds. A similar finding of FTIR peaks around 500 – 850 cm^{-1} was also reported [41].

Adsorption Studies

Effect of pH on the adsorption of ceftriaxone

The pH plays a crucial role in the adsorption process, as it influences the speciation of the adsorbate in solution [42]. Thus, the effect of pH on the adsorption of ceftriaxone was investigated in the current study. As illustrated in Fig. 4, the adsorption efficiency (RE%) of ceftriaxone increased from 82 to 95% as the pH increased from 1 to 2. Beyond pH 2, further increases in pH led to a gradual decline in the adsorption efficiency, reaching a minimum of 80% at pH 8. The lower adsorption efficiency observed at pH 1 may be attributed to electrostatic repulsion between the positively charged ceftriaxone molecules (Fig. S4) and the positively charged surface of the AC. Similarly, the reduced adsorption efficiency at higher pH levels could be due to increased electrostatic repulsion between negatively charged ceftriaxone species and the negatively charged AC surface. The maximum adsorption efficiency of 95%

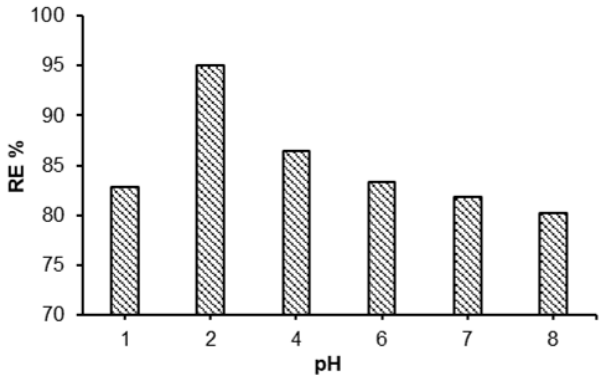

Fig 4. Effect of pH on the adsorption of ceftriaxone. Experimental conditions: pH 2, adsorbent dosage 20 g/L, initial concentration of ceftriaxone 20 mg/L, agitation speed 100 rpm, temperature 298.15 K, and contact time 1 h

was recorded at pH 2, where ceftriaxone predominantly exists in its zwitterionic form, while the AC surface retains a positive charge. This observation suggests that the adsorption of ceftriaxone onto the activated AC was primarily governed by electrostatic attractions between the ceftriaxone and the AC. However, the role played by weak intermolecular interactions, such as van der Waals forces, dipole-dipole interactions, and dispersion forces, cannot be completely ruled out. Comparable results were reported by Yegane Badi et al., who achieved a removal efficiency of 97.18% using Fe_3O_4-modified AC at a slightly acidic pH of 3.14 [43]. Therefore, based on the results in Fig. 4, an optimal removal efficiency of 95% was achieved using a pH of 2.

Effect of concentration of ceftriaxone

The effect of the initial concentration of ceftriaxone on adsorption efficiency was investigated, and the results are presented in Fig. 5. An initial increase in ceftriaxone concentration from 20 to 200 mg/L resulted in an increase in removal efficiency from 95.0 to 97.8%. However, as the concentration further increased from 200 to 1,000 mg/L, the adsorption efficiency declined slightly to 94.5%. The initial rise in efficiency can be attributed to an increased concentration gradient, which enhances the driving force for mass transfer between the liquid phase and the solid adsorbent thereby promoting adsorption [44]. Nevertheless, the mass of AC used (0.1 g) remained constant throughout the experiment, resulting in a fixed number of available adsorption sites. At higher initial concentrations, these sites likely became saturated, limiting further adsorption and causing a decline in removal efficiency. This saturation of adsorption sites, coupled with possible pore blockage, may have contributed to the reduced efficiency observed at higher concentrations [45]. Therefore, based on these findings, an initial concentration of 200 mg/L was determined to be the optimal condition for effective ceftriaxone adsorption in this study.

Effect of dosage on the adsorption of ceftriaxone

The effect of adsorbent dosage on the removal efficiency of ceftriaxone using AC-FPAA-H_3PO_4 was evaluated, as shown in Fig. 6. The results indicated that increasing the dosage from 2 to 20 g/L resulted in only a

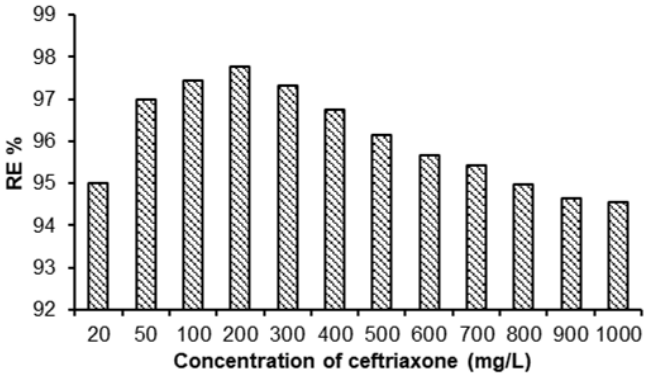

Fig 5. Effect of concentration on the adsorption of ceftriaxone. Experimental conditions: pH 2, temperature 298.15 K, stirring speed 100 rpm, initial concentration of ceftriaxone 20–1000 mg/L, and adsorbent dosage 20 g/L

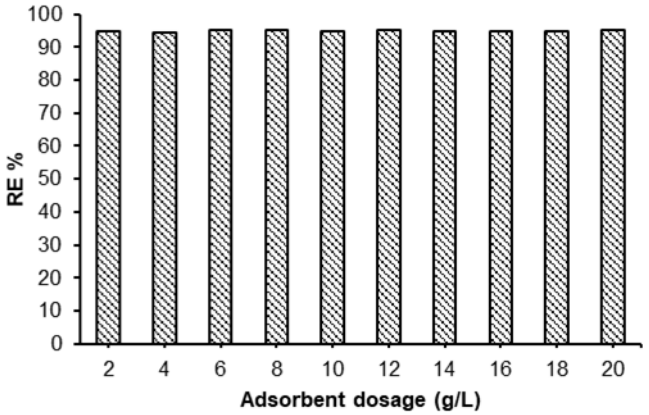

Fig 6. Effect of adsorbent dosage. Experimental conditions: pH 2, initial concentration of ceftriaxone 20 mg/L, stirring speed 100 rpm, temperature 298.15 K, and contact time 1 h

marginal increase in removal efficiency, from 94.67 to 95.05%. This insignificant change suggests that AC-FPAA-H_3PO_4 possesses a high adsorption capacity, enabling it to achieve high removal efficiency even at low dosages. This behavior is likely due to the abundance of adsorption sites within the material, which allows effective removal of the antibiotic even with a minimal amount of adsorbent. These findings contrast with other reported studies, where adsorption efficiency typically increases with dosage up to an optimum point, after which it either plateaus or decreases. For instance, Rinawati et al. reported that the removal efficiencies of ceftriaxone and ciprofloxacin using graphene oxide derived from corn cob increased with adsorbent mass up to optimal levels of 40 and 20 mg, respectively [45]. Similarly, Alawa et al. observed an increase in the removal of ciprofloxacin from water with increasing dosages of biochar derived from agricultural waste biomass, which had BET surface areas of 274 m^2/g (CWS) and 219 m^2/g (AWS) [46]. The high BET surface area of AC-FPAA-H_3PO_4 (1895.646 m^2/g) may explain this deviation from the typical trend. The extensive surface area is likely to provide sufficient active sites to accommodate large quantities of adsorbate, even at low dosages. Therefore, AC-FPAA-H_3PO_4 possesses unique structural features that enable it to maintain high adsorption efficiency regardless of dosage, making it a highly efficient and economical adsorbent.

Effect of temperature on the adsorption of ceftriaxone

Temperature is a parameter that influences adsorption processes, as temperature variations can affect the chemical interactions between the adsorbent and adsorbate. In this study, the removal efficiency of ceftriaxone decreased slightly from 95 to 92% as the temperature increased from 298.15 to 338.15 K (Fig. 7). This decline suggests that the adsorption of ceftriaxone onto AC-FPAA-H_3PO_4 is exothermic in nature, indicating that lower temperatures favor the adsorption process [47]. The reduction in adsorption efficiency at elevated temperatures may be attributed to enhanced desorption and weaker interactions between ceftriaxone and the AC surface. At higher temperatures, the affinity between ceftriaxone and the surrounding solution increases, while its interaction with the adsorbent decreases [48]. These findings are consistent with other reported studies on the adsorption of organic pollutants. For instance, Naghipour et al. observed a similar temperature-dependent decrease in ceftriaxone removal using Fe_2O_3-magnetized kaolin [49]. Comparable behavior has also been reported in the removal of amoxicillin using *Aloe barbadensis* Miller-based bioadsorbents [50] ciprofloxacin removal using biochar derived from agricultural waste [46]. These studies collectively support the conclusion that lower temperatures enhance adsorption efficiency for various organic pollutants.

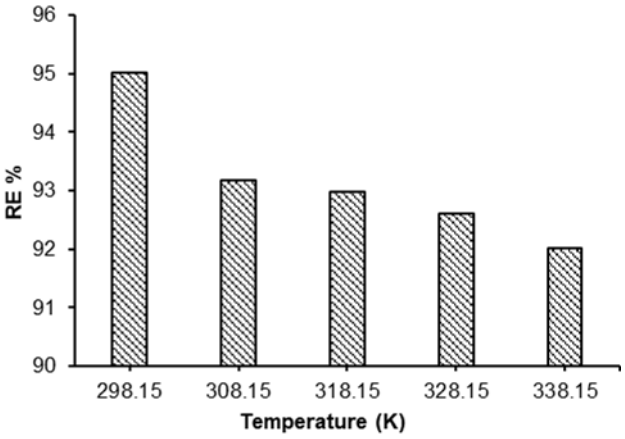

Fig 7. Effect of solution temperature on the adsorption of ceftriaxone. Experimental condition: pH 2, mass of adsorbent-adsorbate solution 20 g/L, initial concentration of ceftriaxone 20 mg/L, stirring speed 100 rpm, and contact time 1 h

Adsorption isotherms for the adsorption of ceftriaxone

The results in Fig. 8 and Table S2 show R^2 values for both Langmuir and Freundlich models of 0.9862 and 0.9833, respectively. The observation suggests that the adsorption of the antibiotic may follow two models. The other parameters related to the Langmuir isotherm model obtained are q_{max} of 72.99 mg/L, K_L of 0.02937 L/g, and R_L of 0.145. The different parameters released to the Freundlich isotherm are the K_F value of 3.119 L/mg and the *n* value of 1.5225. The value of K_L being small (0.02937 L/g), probably indicates the existence

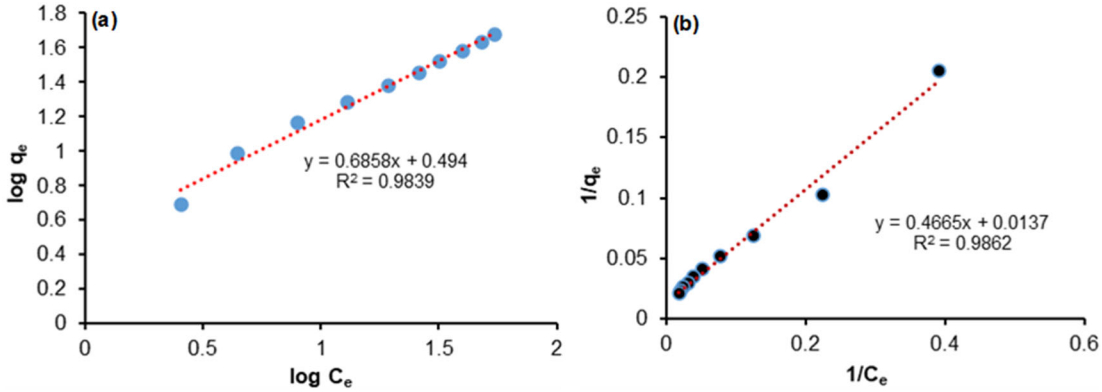

Fig 8. Isothermal models of (a) the Freundlich isothermal model and (b) the Langmuir isotherm model. Experimental conditions: pH 2, temperature 298.15 K, stirring speed 100 rpm, initial concentration of ceftriaxone 20–1000 mg/L, and adsorbent dosage 20 g/L

of weak forces between adsorbent and adsorbate molecules. Additionally, a high value of *n* (1.5225) indicates a stronger interaction between ceftriaxone molecules and AC. Similar findings were previously reported on the removal of industrial dye using AC from the Himalayan char pine biomass [20].

Adsorption kinetics of ceftriaxone antibiotic

The results presented in Fig. 9 and Table S3 show that the R^2 values for the kinetic models were 0.90 for the pseudo-first-order, 0.98 for the pseudo-second-order, 0.90 for the Elovich model, and 0.97 for the Weber's intraparticle diffusion model. The predicted q_e for the pseudo-second-order model was 434.76 mg/g, closely aligning with the experimentally determined q_e value of 435.87 mg/g. The observation suggests that the adsorption is likely governed by chemisorption mechanisms involving valence forces through the sharing or exchange of electrons between ceftriaxone molecules and AC. In contrast, the pseudo-first-order model yielded a predicted q_e of 265.46 mg/g, significantly lower than the experimental value (435.87 mg/g). For the Weber's model, the boundary layer thickness constant (C_i) was calculated as 195.89. The high R^2 values for the pseudo-second-order (0.98) and Weber's intraparticle diffusion model (0.97) probably mean that the adsorption of ceftriaxone onto AC-FPAA-H_3PO_4 likely follows both pseudo-second-order kinetics and intraparticle diffusion mechanisms. Moreover, the close agreement between the predicted and experimental q_e values in the pseudo-second-order model further supports this conclusion. The considerable C_i value (195.89) indicates a significant boundary layer effect, suggesting that external mass transfer resistance may influence the diffusion of ceftriaxone molecules into the pores of the AC. These findings are consistent with previous studies where the adsorption of ceftriaxone onto AC modified with magnetic Fe_3O_4 nanoparticles followed pseudo-second-order kinetics [43].

Thermodynamic Study

The thermodynamic parameters presented in Table 4 and Fig. S5 indicate that the enthalpy change (ΔH) and entropy change (ΔS) for the adsorption of ceftriaxone using AC-FPAA-H_3PO_4 were −4.4292 kJ mol^{-1} and 7.691 J mol^{-1} K^{-1}, respectively. The Gibbs free energy changes (ΔG) at various temperatures 298.15, 308.15, 318.15, 328.15, and 338.15 K were found to be −6.8270, −6.6946, −6.8359, −6.8917, and −7.1390 kJ mol^{-1}, respectively. The average ΔG value of −6.7980 kJ mol^{-1} across these temperatures suggests that the adsorption process occurs spontaneously under the studied conditions.

The negative value of ΔH confirms that the adsorption process is exothermic. In contrast, the positive value of ΔS indicates an increase in randomness at the solid-solution interface during the adsorption. Additionally, the positive ΔS also suggests a high affinity of the AC for ceftriaxone molecules, as greater disorder

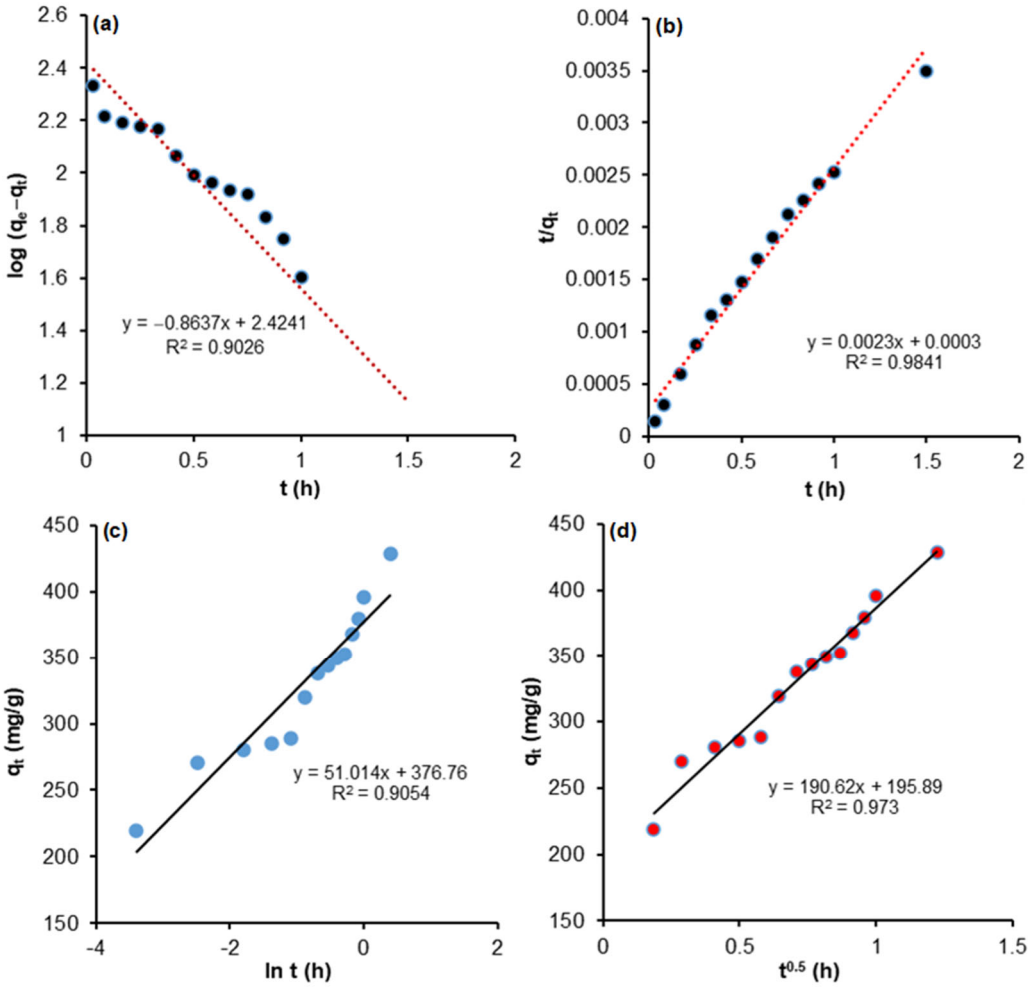

Fig 9. Kinetics models: (a) pseudo-first-order, (b) pseudo-second-order, (c) Elovich, and (d) Weber's model. Experimental conditions: pH 2, adsorbent dosage 1 g/L, initial concentration of ceftriaxone solution 500 mg/L, stirring speed 100 rpm, and temperature 298.15 K

Table 4. Summary of thermodynamic parameters

Temperature (K)	ΔG (kJ mol^{-1})	ΔH (kJ mol^{-1})	ΔS (J mol^{-1} K^{-1})
298.15	−6.82709		
308.15	−6.69460		
318.15	−6.83593	−4.4292	7.69128
328.15	−6.89166		
338.15	−7.13898		

typically reflects favorable interactions between adsorbates and adsorbents. These findings are consistent with previous studies on the thermodynamics of adsorption processes [51]. Overall, the thermodynamic data demonstrate that ceftriaxone removal using AC-FPAA-H_3PO_4 is both feasible and favorable at room temperature, highlighting its potential for industrial-scale application without the need for extensive temperature regulation.

Application of AC-FPAA-H_3PO_4 in Real Water Samples

Real water samples used in this experiment were collected from the Ngerengere River near Solomon Mahlangu Campus in Mazimbu and from a well at the Free Pentecostal Church of Tanzania (FPCT)-Kihonda Magorofani, in Morogoro Municipal, Tanzania. Before the adsorption experiments, the conductivity and pH of the water samples were measured and recorded (Table S4). The results (Fig. S6) showed removal efficiencies of 99.36% for river water and 96.92% for well water in the

Table 5. Summary of comparison of the removal efficiency of ceftriaxone using AC-FPAA-H_3PO_4 with other adsorbents

Adsorbent	pH	Adsorbate concentration	Kinetic	RE (%)	Reference
AC-FPAA-H_3PO_4	2	200 mg/L	PSO	97.8	This study
Saccharomyces cerevisiae	6	10 mg/L	PSO	78.0	[52]
Graphene oxide	8	25 mg/L	-	95.9	[53]
Graphene oxide from corn cob	4	14 mg/L	-	47.0	[45]
AC with magnetic Fe_3O_4 nanoparticle composite	3	10 mg/L	PSO	97.2	[43]
Chitosan/graphene oxide nanocomposite functionalized with zirconium	7.5	20 mg/L	PSO	97.1	[54]
Pseudomonas pudica biomass	7	50 mg/L	-	50.0	[55]
AC derived from agricultural product waste	7	1.77×10^{-3} mol/L	PSO	84.0	[18]
Assembled composite of nano-titanium oxide/chitosan/nano-bentonite	5	-	PSO	93.5	[56]

*PSO: pseudo-second-order

first cycle, indicating that coexisting constituents in real water samples had minimal impact on AC-FPAA-H_3PO_4's adsorption efficiency. The reusability was evaluated to assess practical applicability and reduce costs/environmental impact. After each cycle, the spent adsorbent was centrifuged, decanted, and dried at 90 °C for 1 h. Fig. S6 also showed a decline in removal efficiency with increasing cycles, from 99.36 to 88.05% for river water and from 96.92 to 90.44% for well water. This reduction likely resulted from progressive pore blockage by accumulated ceftriaxone molecules, suggesting multilayer formation consistent with earlier observations in the current study. Although AC-FPAA-H_3PO_4 remained effective through five reuse cycles, adding a desorption step could potentially improve long-term performance; however, adsorbent loss during regeneration may impact efficiency.

Comparability of AC-FPAA with Other Adsorbents

The performance of AC-FPAA-H_3PO_4 was compared with other adsorbents reported in the literature (Table 5). The AC-FPAA-H_3PO_4 demonstrated the highest ceftriaxone removal efficiency (97.8%), even at a high initial concentration of 200 mg/L. Comparable efficiencies were observed for AC modified with magnetic Fe_3O_4 nanoparticles (97.18%) and a chitosan/graphene oxide nanocomposite functionalized with zirconium (97.1%). While these values were similar, AC-FPAA-H_3PO_4 still exhibited superior performance. Other adsorbents showed significantly lower removal efficiencies: graphene oxide from corn cob (47%), *Pseudomonas pudica* biomass (50%), *Saccharomyces cerevisiae* biomass (78%), agricultural waste-derived AC (84%), nano-titanium oxide/chitosan/nano-bentonite composite (93.5%), and unmodified graphene oxide (95.87%). The enhanced adsorption capability of AC-FPAA-H_3PO_4 is likely due to its exceptionally high specific surface area (1,895.646 m^2/g), which provides abundant active sites and allows for the accommodation of a greater number of ceftriaxone molecules. Thus, AC-FPAA-H_3PO_4 ranks among the most effective adsorbents for ceftriaxone removal from aqueous solutions. However, post-synthesis surface modifications, such as amination or magnetic functionalization, can be employed to enhance binding and reusability. The proposed techniques may also allow the adsorbent to meet specific environmental remediation needs.

■ CONCLUSION

This study successfully synthesized micro-mesoporous AC (AC-FPAA-H_3PO_4) from *A. angustifolium* fruit shells via H_3PO_4 activation (4 M, 600 °C, 1 h) for the removal of ceftriaxone. The AC exhibited a high surface area (1895.646 m^2/g) with a removal efficiency of 97.8% at pH 2, an initial concentration of 200 mg/L, and a temperature of 298.15 K within 1 h. The adsorption process followed both Langmuir (monolayer, $R^2 = 0.9862$) and Freundlich (multilayer, $R^2 = 0.9833$) isotherms, with kinetics best described by the pseudo-second-order ($R^2 = 0.982$) and

intraparticle diffusion ($R^2 = 0.973$) models. Thermodynamics confirmed a spontaneous ($\Delta G = -6.80$ kJ mol^{-1}), exothermic ($\Delta H = -4.43$ kJ mol^{-1}), and entropy-driven ($\Delta S = 7.69$ J mol^{-1} K^{-1}) process. The AC-FPAA-H_3PO_4 demonstrated high efficacy in real water matrices (99.36% river water, and 96.92% well water) and maintained significant removal after 5 cycles without the regeneration of active sites (88.05% river water, and 90.44% well water). This novel, reusable adsorbent offers a promising, low-cost solution for removing organic contaminants in water treatment.

■ ACKNOWLEDGMENTS

The study was funded by the Sokoine University of Agriculture.

■ CONFLICT OF INTEREST

On behalf of all authors, the corresponding author states that there is no conflict of interest.

■ AUTHOR CONTRIBUTIONS

All authors have accepted responsibility for the entire content of this manuscript and consented to its submission to the journal, reviewed all the results, and approved the final version of the manuscript. Baraka Alfaksad Kasazi: conceptualization, methodology, formal analysis, investigation, writing original draft preparation. Alinanuswe Joel Mwakalesi: conceptualization, methodology, formal analysis, review, and editing. Emmy Solomon Lema: investigation, methodology, review, and editing. All authors read and agreed to the final version of this manuscript.

■ REFERENCES

[1] Osuoha, J.O., Anyanwu, B.O., and Ejileugha, C., 2023, Pharmaceuticals and personal care products as emerging contaminants: Need for combined treatment strategy, *J. Hazard. Mater. Adv.*, 9**,** 100206.

[2] Klein, E.Y., Impalli, I., Poleon, S., Denoel, P., Cipriano, M., van Boeckel, T.P., Pecetta, S., Bloom, D.E., and Nandi, A., 2024, Global trends in antibiotic consumption during 2016–2023 and future projections through 2030, *Proc. Natl. Acad. Sci. U. S. A.*, 121 (49), e2411919121.

[3] Wada, O.Z., and Olawade, D.B., 2025, Recent occurrence of pharmaceuticals in freshwater, emerging treatment technologies, and future considerations: A review, *Chemosphere*, 374, 144153.

[4] Nguyen, M.K., Lin, C., Nguyen, H.L., Hung, N.T.Q., La, D.D., Nguyen, X.H., Chang, S.W., Chung, W.J., and Nguyen, D.D., 2023, Occurrence, fate, and potential risk of pharmaceutical pollutants in agriculture: Challenges and environmentally friendly solutions, *Sci. Total Environ.*, 899, 165323.

[5] Zheng, S., Wang, Y., Chen, C., Zhou, X., Liu, Y., Yang, J., Geng, Q., Chen, G., Ding, Y., and Yang, F., 2022, Current progress in natural degradation and enhanced removal techniques of antibiotics in the environment: A review, *Int J Environ Res Public Health.*, 19 (17),10919.

[6] Akhter, S., Bhat, M.A., Ahmed, S., and Siddiqui, W.A., 2024, Antibiotic residue contamination in the aquatic environment, sources and associated potential health risks, *Environ. Geochem. Health*, 46 (10), 387.

[7] Parvin, F., and Tareq, S.M., 2021, Impact of landfill leachate contamination on surface and groundwater of Bangladesh: A systematic review and possible public health risks assessment, *Appl. Water Sci.*, 11 (6), 100.

[8] Bilal, M., Mehmood, S., Rasheed, T., and Iqbal, H.M.N., 2020, Antibiotics traces in the aquatic environment: Persistence and adverse environmental impact, *Curr. Opin. Environ. Sci. Health*, 13, 68–74.

[9] Mandal, D., 2024, Various antibiotic contamination in natural sources: Effects on environment including animals and humans, *Orient. J. Chem.*, 40, 342–354.

[10] Barathan, M., Ng, S.L., Lokanathan, Y., Ng, M.H., and Law, J.X., 2024, Unseen weapons: Bacterial extracellular vesicles and the spread of antibiotic resistance in aquatic environments, *Int. J. Mol. Sci.*, 25 (6), 3080.

[11] Baralla, E., Demontis, M., Dessì, F., and Varoni, M., 2021, An overview of antibiotics as emerging contaminants: Occurrence in bivalves as biomonitoring organisms, *Animals*, 11 (11), 3239.

[12] Bittner, M.J., Dworzack, D.L., Preheim, L.C., Tofte, R.W., and Crossley, K.B., 1983, Ceftriaxone therapy of serious bacterial infections in adults, *Antimicrob. Agents Chemother.*, 23 (2), 261–266.

[13] Roubaud-Baudron, C., Fauchon, H., Stanke-Labesque, F., Paccalin, M., Breilh, D., Grégoire, N., Forestier, E., Ferry, T., Gavazzi, G., and Goutelle, S., 2025, Pharmacokinetics of subcutaneous and intravenous ceftriaxone in an older population: The PhASAge study, *Open Forum Infect. Dis.*, 12 (6), ofaf313.

[14] Al-Sudani, I., Al-Razzaq, H.A., Audy, R., and Al-Khayat, A., 2024, Risk of ceftriaxone (antibiotic) in the Tigris River water, Iraq, *Asian J. Water, Environ. Pollut.*, 21 (1), 81–87.

[15] Karungamye, P., Rugaika, A., Mtei, K., and Machunda, R., 2022, A review of methods for removal of ceftriaxone from wastewater, *J. Xenobiot.*, 12 (3), 223–235.

[16] Gelaw, L.Y., Bitew, A.A., Gashey, E.M., and Ademe, M.N., 2022, Ceftriaxone resistance among patients at GAMBY teaching general hospital, *Sci. Rep*., 12 (1), 12000.

[17] Dimbo, D., Abewaa, M., Adino, E., Mangistu, A., Takele, T., Oro, A., and Rangaraju, M., 2024, Methylene blue adsorption from aqueous solution using activated carbon of *Spathodea campanulata*, *Results Eng.*, 21, 110910.

[18] Alibrahim, K.A., 2023, Enhanced adsorption of ceftriaxone antibiotics from water by activated carbon derived from agriculture products waste, *J. Mol. Recognit.*, 36 (7), e3016.

[19] Nandikes, G., Nguyen, A.H., Siddiqui, S.I., and Oh, S., 2025, Sustainable water treatment using agricultural residue adsorbents: Evaluating efficacy and life cycle impacts, *J. Ind. Eng. Chem.*, 149, 889–900.

[20] Prasad, B., Goswami, R., Mishra, A., Gill, F.S., Juyal, S., Asrani, A., Jain, A., Sahu, R., Gupta, M.K., Bajaj, M., and Zaitsev, I., 2024, Assessment of carbonized Himalayan Chir pine biomass as an eco-friendly adsorbent for effective removal of industrial dyes, *Sci. Rep.*, 14 (1), 15694.

[21] Kumar, P., Nashath Omer, S., Redy, M.M., Saravanan, P., Rajeshkannan, R., Rajasimman, M., Shanmugam, V.K., Kamyab, H., Gupta, V.K., and Vasseghian, Y., 2024, Exploring the role of activated charcoal from lignocellulosic biomass wastes for sustainable water treatment, *J. Energy Inst.*, 114, 101626.

[22] Al-Gheethi, A.A., Azhar, Q.M., Senthil Kumar, P., Yusuf, A.A., Al-Buriahi, A.K., Radin Mohamed, R.M.S., and Al-shaibani, M.M., 2022, Sustainable approaches for removing rhodamine B dye using agricultural waste adsorbents: A review, *Chemosphere*, 287 (Pt. 2), 132080.

[23] Topare, N.S., and Wadgaonkar, V.S., 2023, A review on application of low-cost adsorbents for heavy metals removal from wastewater, *Mater. Today: Proc.*, 77, 8–18.

[24] Tugume, P., and Nyakoojo, C., 2020, Traditional use of wild edible plants in the communities adjacent to Mabira Central Forest Reserve, Uganda, *Ethnobot. Res. Appl.*, 20, 1–14.

[25] Tayyab, M., Noman, A., Islam, W., Waheed, S., Arafat, Y., Ali, F., Zaynab, M., Lin, S., Zhang, H., and Khan, D., 2018, Bioethanol production from lignocellulosic biomass by environment-friendly pretreatment methods: A review, *Appl. Ecol. Environ. Res.*, 16 (1), 225–249.

[26] Islam, M.A., Nazal, M.K., Akinpelu, A.A., Sajid, M., Alhussain, N.A., and Ilyas, M., 2024, High performance adsorptive removal of emerging contaminant paracetamol using a sustainable biobased mesoporous activated carbon prepared from palm leaves waste, *J. Anal. Appl. Pyrolysis*, 180, 106546.

[27] Ekpete, O.A., Marcus, A.C., and Osi, V., 2017, Preparation and characterization of activated carbon obtained from plantain (*Musa paradisiaca*) fruit stem, *J. Chem.*, 2017 (1), 8635615.

[28] Ceyhan, A.A., Şahin, Ö., Baytar, O., and Saka, C., 2013, Surface and porous characterization of activated carbon prepared from pyrolysis of biomass by two-stage procedure at low activation temperature and it's the adsorption of iodine, *J. Anal. Appl. Pyrolysis*, 104, 378–383.

[29] Divya, M.P., Krishnamoorthi, S., Ravi, R., Jenner, V.G., Baranidharan, K., Raveendran, M., and

Hemalatha, P., 2025, Preparation and characterization of activated carbon from commercially important bamboo species in north eastern India, *Adv. Bamboo Sci.*, 11, 100148.

[30] Zulkania, A., Hanum, G.F., and Sri Rezki, A., 2018, The potential of activated carbon derived from bio-char waste of bio-oil pyrolysis as adsorbent, *MATEC Web Conf.*, 154, 01029.

[31] Parmanbek, N., Sütekin, D.S., Barsbay, M., Mashentseva, A.A., Zheltov, D.A., Aimanova, N.A., Jakupova, Z.Y., and Zdorovets, M.V., 2022, Hybrid PET track-etched membranes grafted by well-defined poly(2-(dimethylamino)ethyl methacrylate) brushes and loaded with silver nanoparticles for the removal of As(III), *Polymers*, 14 (19), 4026.

[32] Jawad, A.H., Mamat, N.F.H., Abdullah, M.F., and Ismail, K., 2017, Adsorption of methylene blue onto acid-treated mango peels: kinetic, equilibrium and thermodynamic study, *Desalin. Water Treat.*, 59, 210–219.

[33] Ruvubu, S.B., and Roy, I., 2025, Innovative nanocomposites for pollutant capture: Adsorption of rhodamine B dye using polyaniline-coated chitosan trisodium citrate nanocomposites, *Int. J. Biol. Macromol.*, 292, 139293.

[34] Selmi, T., Gentil, S., Fierro, V., and Celzard, A., 2024, Key factors in the selection, functionalization and regeneration of activated carbon for the removal of the most common micropollutants in drinking water, *J. Environ. Chem. Eng.*, 12 (4), 113105.

[35] Alsuhaibani, A.M., Refat, M.S., Adam, A.M.A., El-Desouky, M.G., and El-Bindary, A.A., 2023, Enhanced adsorption of ceftriaxone antibiotics from water by mesoporous copper oxide nanosphere, *Desalin. Water Treat.*, 281, 234–248.

[36] Singh, N., Sharma, D., Thakur, M., and Dan, A., 2025, Zinc oxide-loaded chitosan-graphene oxide hydrogel nanocomposite as a potential catalyst for photocatalytic dye degradation, *Int. J. Biol. Macromol.*, 308, 142424.

[37] Islam, M.A., Nazal, M.K., Akinpelu, A.A., Sajid, M., Alhussain, N.A., Billah, R.E.K., and Bahsis, L., 2024, Novel activated carbon derived from a sustainable and low-cost palm leaves biomass waste for tetracycline removal: Adsorbent preparation, adsorption mechanisms and real application, *Diamond Relat. Mater.*, 147, 111375.

[38] Balasubramaniam, N., and Louise, I.S.Y., 2025, Isotherm and kinetic studies of malachite green by NaOH-activated carbon made from apple waste, *Indones. J. Chem.*, 25 (4), 1113–1131.

[39] Pavia, D.L., Lampman, G.M., and Kriz, G.S., 2001, *Introduction to Spectroscopy: A Guide for Students of Organic Chemistry*, Brooks/Cole, Belmont, CA, US.

[40] Tran, T.N.D., Tran, T.T., Hoang, B.N., Lam, V.T., and Ngo, T.C.Q., 2024, Synthesis of activated carbon from dragon fruit peel for adsorption of methyl blue, *Indones. J. Chem.*, 24 (6), 1602–1614.

[41] Maulina, S., and Anwari, F.N., 2019, Comparing characteristics of charcoal and activated carbon from oil palm fronds, *IOP Conf. Ser.: Earth Environ. Sci.*, 305, 012059.

[42] Onditi, M., Adelodun, A.A., Changamu, E.O., and Ngila, J.C., 2016, Removal of Pb^{2+} and Cd^{2+} from drinking water using polysaccharide extract isolated from cactus pads (*Opuntia ficus indica*), *J. Appl. Polym. Sci.*, 133 (38), 43913.

[43] Yegane Badi, M., Azari, A., Pasalari, H., Esrafili, A., and Farzadkia, M., 2018, Modification of activated carbon with magnetic Fe_3O_4 nanoparticle composite for removal of ceftriaxone from aquatic solutions, *J. Mol. Liq.*, 261, 146–154.

[44] Luoyang, Y., Wang, H., Yong, W., Li, J., Li, X., Shenghu, H., Ying, N., and Guotao, Z., 2024, Blue coke-based activated carbon adsorbents: Insights into the efficiency and mechanism of methyl blue removal, *Arabian J. Chem.*, 17 (9), 105898.

[45] Rinawati, R., Rahmawati, A., Muthia, D.R., Imelda, M.D., Latief, F.H., Mohamad, S., and Kiswandono, A.A., 2024, Removal of ceftriaxone and ciprofloxacin antibiotics from aqueous solutions using graphene oxide derived from corn cob, *Global J. Environ. Sci. Manage.*, 10 (2), 573–588.

[46] Alawa, B., Singh, S., Chakma, S., Kishor, R., Stålsby Lundborg, C., and Diwan, V., 2025, Development of novel biochar adsorbent using agricultural waste biomass for enhanced removal of ciprofloxacin from

water: Insights into the isotherm, kinetics, and thermodynamic analysis, *Chemosphere*, 375, 144252.

[47] Abdel-Aziz, M.H., El-Ashtoukhy, E.Z., Bassyouni, M., Al-Hossainy, A.F., Fawzy, E.M., Abdel-Hamid, S.M., and Zoromba, M.S., 2021, DFT and experimental study on adsorption of dyes on activated carbon prepared from apple leaves, *Carbon Lett.*, 31 (5), 863–878.

[48] Foo, K.Y., and Hameed, B.H., 2010, An overview of dye removal via activated carbon adsorption process, *Desalin. Water Treat.*, 19 (1), 255–274.

[49] Naghipour, D., Taghavi, K., Jaafari, J., Hashim, K.S., Javan Mahjoub Doust, F., and Mahjoub Doust, M.J., 2024, Evaluation of the efficacy of Fe_2O_3 magnetised kaolin: Simultaneous removal of ceftriaxone and cefixime from aqueous media, *Int. J. Environ. Anal. Chem.*, 104 (17), 4928–4945.

[50] Getenew, K., and Misganaw, A., 2024, Removal of amoxicillin from contaminated water using *Aloe barbadensis* miller bio-adsorbent, *Results Eng.*, 22, 102081.

[51] Liu, H.Q., Xu, X., Wu, Z.H., Wei, G.X., and Sun, L., 2015, Removal of heavy metals from aqueous solution using biochar derived from biomass and sewage sludge, *Appl. Mech. Mater.*, 768, 89–95.

[52] Samarghandi, M.R., Asgari, G., Shokoohi, R., Dargahi, A., Golrokhi, M., Faraji, H., and Arabkouhsar, A., 2019, Efficiency of *Saccharomyces cerevisiae* in ceftriaxone removal from aquatic environments: Kinetic, isotherm of absorption and thermodynamics study, *J. Health*, 10 (3), 270–286.

[53] Li, Z., Zhang, S., Zhu, G., and Xing, J., 2024, Use of graphene oxide for the removal of norfloxacin and ceftriaxone antibiotics from aqueous solution: Process optimization using response surface approach, *Front. Environ. Sci.*, 12, 1436848.

[54] Jafarzadeh, N., Jaafari, J., Moslemzadeh, M., and Taghavi, K., 2025, A novel chitosan/graphene oxide nanocomposite functionalized with zirconium to remove dexamethasone and ceftriaxone from aqueous solutions: Response surface methodology, isotherm, kinetic and thermodynamic, *J. Water Process Eng.*, 69, 106722.

[55] Bozorginia, S., Jaafari, J., Taghavi, K., Ashrafi, S.D., Roohbakhsh, E., and Naghipour, D., 2023, Biosorption of ceftriaxone antibiotic by *Pseudomonas putida* from aqueous solutions, *Int. J. Environ. Anal. Chem.*, 103 (9), 2067–2081.

[56] Mahmoud, M.E., El-Ghanam, A.M., Mohamed, R.H.A., and Saad, S.R., 2020, Enhanced adsorption of levofloxacin and ceftriaxone antibiotics from water by assembled composite of nanotitanium oxide/chitosan/nano-bentonite, *Mater. Sci. Eng., C*, 108, 110199.